

Ultrastable optical clock with two cold-atom ensembles

M. Schioppo^{1,2,3}, R. C. Brown¹, W. F. McGrew^{1,2}, N. Hinkley^{1,2}, R. J. Fasano^{1,2}, K. Beloy¹, T. H. Yoon^{1,4}, G. Milani^{1,5,6}, D. Nicolodi¹, J. A. Sherman¹, N. B. Phillips¹, C. W. Oates¹ and A. D. Ludlow^{1*}

Atomic clocks based on optical transitions are the most stable, and therefore precise, timekeepers available. These clocks operate by alternating intervals of atomic interrogation with the ‘dead’ time required for quantum state preparation and readout. This non-continuous interrogation of the atom system results in the Dick effect, an aliasing of frequency noise from the laser interrogating the atomic transition^{1,2}. Despite recent advances in optical clock stability that have been achieved by improving laser coherence, the Dick effect has continually limited the performance of optical clocks. Here we implement a robust solution to overcome this limitation: a zero-dead-time optical clock that is based on the interleaved interrogation of two cold-atom ensembles³. This clock exhibits vanishingly small Dick noise, thereby achieving an unprecedented fractional frequency instability assessed to be $6 \times 10^{-17}/\sqrt{\tau}$ for an averaging time τ in seconds. We also consider alternate dual-atom-ensemble schemes to extend laser coherence and reduce the standard quantum limit of clock stability, achieving a spectroscopy line quality factor of $Q > 4 \times 10^{15}$.

Optical atomic clocks operate by tuning the frequency of a laser (optical local oscillator, OLO) into resonance with a narrowband electronic transition in an atomic system^{4,5}. By so doing, the intrinsic ‘ticking’ rate of the atom ($\sim 10^{15}$ Hz), given by the phase evolution of the electronic wave function, is transferred to the laser field for use as a timebase. Any noise influencing this transfer process compromises the resulting laser frequency stability, and thus the timekeeping precision. Optical clock stability is typically compromised by two classes of noise: atomic detection noise and OLO-induced noise.

Atomic detection noise encapsulates the processes associated with the measurement of atomic states. The fundamental limit arises from quantum projection noise (QPN), as an atom’s state collapses non-deterministically to a particular eigenstate⁶. Photon shot noise associated with the measurement technique (for example, laser-induced fluorescence) also contributes, as does technical noise derived from fluctuations in: (i) the optical field used to measure the atomic state; (ii) the number of atoms participating; and (iii) the opto-electronic signal ultimately being measured. Adding these noise terms, a simplified expression for the fractional clock instability resulting from atomic detection can be formed:

$$\sigma_{\text{atom}}(\tau) \approx \frac{1}{\pi Q} \sqrt{\frac{T_C}{\tau} \sqrt{\frac{1}{N} + \frac{1}{Nn}} + \delta_{\text{det}}^2} \quad (1)$$

where Q is the line quality factor (ratio of electronic transition frequency to linewidth), T_C is the clock cycle time, N is the number of

atoms being interrogated with n photons detected per atom and δ_{det} characterizes the technical detection fluctuations that manifest as a fractional variation in the normalized atomic excitation. For the optical lattice clock considered here, typical operating conditions are $T_C = 530$ ms, $Q \approx 2.7 \times 10^{14}$, $N \approx 5,000 - 10,000$ and $n \gg 1$. Under these conditions the fundamental limit due to QPN yields a potential clock instability of $1 \times 10^{-17}/\sqrt{\tau}$, making the optical lattice clock a powerful tool for a variety of precision tests of fundamental constants⁴, general relativity⁷ and even searches for dark matter^{8,9}.

Regrettably, atomic detection noise is typically exceeded by noise that originates from the OLO. During quantum state preparation and readout, OLO frequency fluctuations are not observed by the atomic system. Consequently, fluctuations at harmonic frequencies of $1/T_C$ are aliased by this periodic atomic interrogation. This aliased noise, known as Dick noise¹, is then improperly compensated in the laser tuning process, compromising the stability of the optical clock. The Dick instability for a clock duty cycle near 50% can be approximated as^{2,4}:

$$\sigma_{\text{Dick}}(\tau) \approx \frac{\sigma_{\text{OLO}}}{\sqrt{2 \ln 2}} \sqrt{\frac{T_C}{\tau} \left| \frac{\sin(\pi T_F/T_C)}{\pi T_F/T_C} \right|} \quad (2)$$

where T_F is the Ramsey free-evolution-time and σ_{OLO} is the OLO flicker frequency instability. The OLO usually comprises a laser that is pre-stabilized to an isolated, high-finesse Fabry–Pérot cavity. For typical operating conditions of current lattice clocks and a state-of-the-art thermal-noise-limited cavity, Dick noise remains dominant over the QPN limit. Consequently, optical clock stability is mostly set by the OLO rather than the atomic system. Advances in the stability of optical clocks have thus been realized using iteratively higher performing OLOs^{10–19}. In some cases, the OLO becomes experimentally more complex than the atomic system it interrogates, challenging future applications of optical clocks outside the laboratory²⁰, including relativistic geodesy^{21,22} and space-borne tests of general relativity²³.

Here we implement two optical-lattice-trapped cold-ytterbium systems that are interrogated by a shared OLO (Fig. 1 and Methods). When operated independently, these systems form two conventional optical clocks, each composed of one cold atom system that is interrogated by the OLO. Table 1 shows the instability budgets of these clocks. Technical fluctuations in the atomic detection measured to be $\delta_{\text{det}} \approx 3\%$ contribute an instability of $3 \times 10^{-17}/\sqrt{\tau}$. Additional noise σ_{phase} arising from length fluctuations in the optical path between the OLO and the two atomic systems is also considered.

¹National Institute of Standards and Technology, 325 Broadway, Boulder, Colorado 80305, USA. ²Department of Physics, University of Colorado, Boulder, Colorado 80309, USA. ³Institut für Experimentalphysik, Heinrich-Heine-Universität Düsseldorf, 40225 Düsseldorf, Germany. ⁴Department of Physics, Korea University, 145 Anam-ro, Seongbuk-gu, Seoul 02841, South Korea. ⁵Instituto Nazionale di Ricerca Metrologica, Strada delle Cacce 91, 10135 Torino, Italy. ⁶Politecnico di Torino, Corso duca degli Abruzzi 24, 10125 Torino, Italy. *e-mail: andrew.ludlow@nist.gov

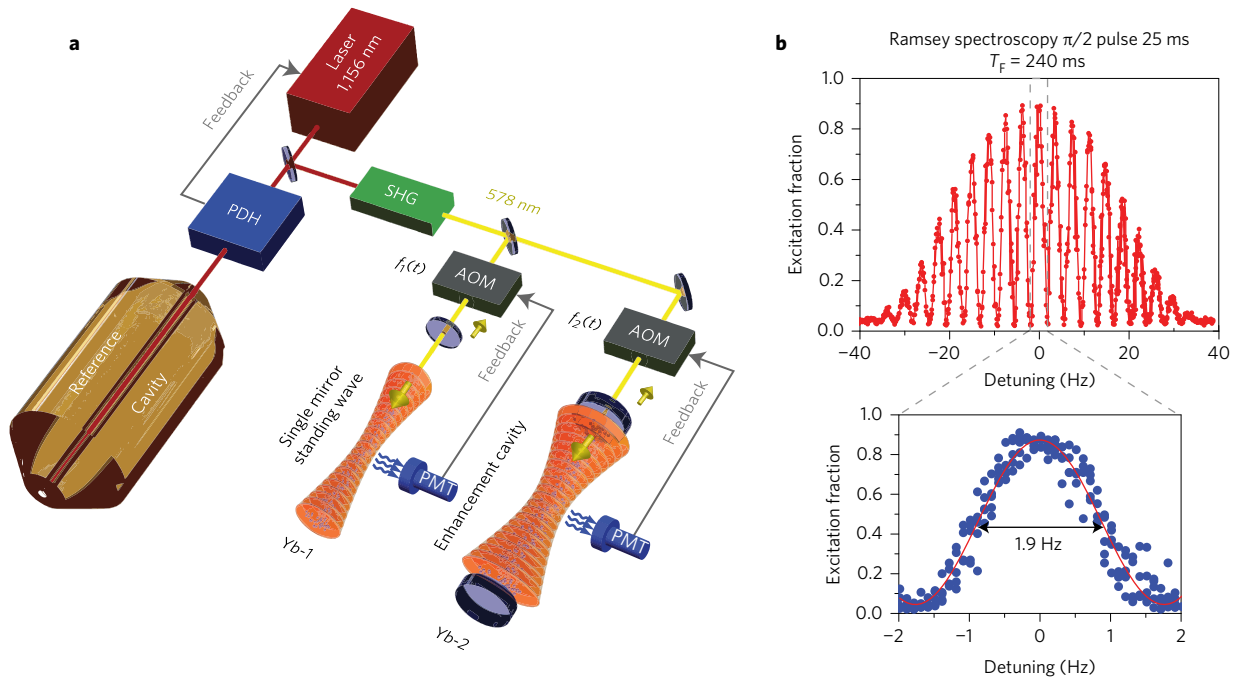


Figure 1 | Experimental scheme. **a**, Laser light generated by a quantum dot laser at 1,156 nm is Pound-Drever-Hall (PDH) stabilized to a high-finesse optical cavity, frequency doubled through a second-harmonic-generation (SHG) crystal waveguide to reach the atomic clock transition at 578 nm, split between two atomic ensembles (Yb-1 and Yb-2) and tuned into resonance by two independent frequency shifters (AOMs) operating at frequencies $f_1(t)$ and $f_2(t)$, respectively, as a function of time, t . Resonance with the atomic transition is detected by measuring the atomic fluorescence collected on a photo-multiplier (PMT). At the lattice, a fraction of the light at 578 nm is reflected back to interferometrically detect and remove environmental phase noise that is accumulated in the optical path from the cavity to the lattice. **b**, Ramsey spectrum under typical conditions used to frequency-stabilize the clock laser on the atomic transition. Each fringe has a linewidth of 1.9 Hz, with the central component having a contrast >90%. The spectrum shown was not subjected to averaging.

Measurement between the two atomic systems allows for the direct characterization of their performance given by the underlying noise processes. To highlight the importance of Dick noise, we first perform atomic interrogation in an antisynchronized fashion so that the Ramsey free-evolution-time of one system ($T_F = 240$ ms) overlaps the dead time of the other system (Fig. 2a). This ensures maximum sensitivity to the OLO aliasing process. Given the measured flicker frequency instability of our OLO $\leq 1.5 \times 10^{-16}$, the Dick effect for one system is calculated to be $7 \times 10^{-17}/\sqrt{\tau}$. As displayed in Fig. 2a, in this antisynchronized configuration we measure a single-clock instability of $< 1.4 \times 10^{-16}/\sqrt{\tau}$ (see Table 1 and Methods). This demonstrates that use of a state-of-the-art OLO affords unprecedented optical clock stability^{10–15}. Nevertheless, Dick noise continues to dominate the achieved level of performance. Improvements could be made by enhancing OLO coherence, which also affords longer spectroscopy times. An alternative approach reduces dead time with multiple non-destructive measurements that

are repeated after a single period of atomic preparation²⁴. However, Fig. 3 highlights that in both of these cases and for the conditions considered here, performance is still limited above QPN.

A distinct optical clock architecture that combines two atomic ensembles (Yb-1 and Yb-2) to form a single clock has the potential to nearly eliminate aliased OLO noise^{3,11,25}. Using the same antisynchronized interrogation, measurements of the atomic response of each system are now combined to derive a single, shared error signal and frequency correction to the OLO. The combined atomic systems provide quasicontinuous monitoring of the OLO frequency, which significantly reduces the aliasing effect. This can be described quantitatively with the sensitivity function (Fig. 2b), defining the atomic response to OLO frequency fluctuations over time. Each atomic ensemble exhibits unit sensitivity during its Ramsey free-evolution-time and zero sensitivity during its dead-time. When two cold-atom-ensembles are merged together to yield one zero-dead-time (ZDT) optical clock, the composite sensitivity remains constant at all times except for small variations during the short Ramsey pulses, and thus provides a significantly reduced susceptibility to the OLO frequency noise at harmonics of $1/T_C$. Figure 2b shows the shared-frequency-correction used in this ZDT stabilization process. For the experimental conditions above, the Dick instability is computed to be $< 3 \times 10^{-18}/\sqrt{\tau}$, now significantly below QPN. Further reductions could be realized by fine adjustment of the relative timing and shape of the Ramsey pulses to achieve an even more uniform composite-sensitivity-function³.

A direct measurement of the ZDT clock instability would be possible by comparing two independent ZDT systems, each composed of dual cold-atom ensembles (see Supplementary Information). Lacking the four atomic ensembles needed for such a measurement, we evaluate clock stability with an alternative scheme using the synchronized interrogation of the two separate atomic systems with a shared OLO¹⁶, as shown in Fig. 2c. Owing to the dead time and the corresponding

Table 1 | Instability budgets for different operational configurations.

	Antisynchronized	Synchronized	ZDT
σ_{QPN}	1	1	$1/\sqrt{2}$
$\sigma_{\text{technical}}$	3	3	$3/\sqrt{2}$
σ_{phase}	2	2	2
σ_{Dick}	$7\sqrt{2}$	Common-mode rejected	< 0.3
Estimated σ_{Total}	11	4	3
Experimental σ_{Total}	14	8	6

All values are in units of $10^{-17}/\sqrt{\tau}$. Contributions to a single system from quantum-projection noise, technical noise in the detection, residual noise from phase-stabilization of the clock laser and the Dick effect are included, respectively. The total gives the quadrature sum of the different estimated noise terms (see Methods). Note that Dick noise levels can be found in Fig. 3b for $T_F = 240$ ms. The bottom row also lists the experimentally assessed instabilities, which are in reasonable agreement with their simple estimates.

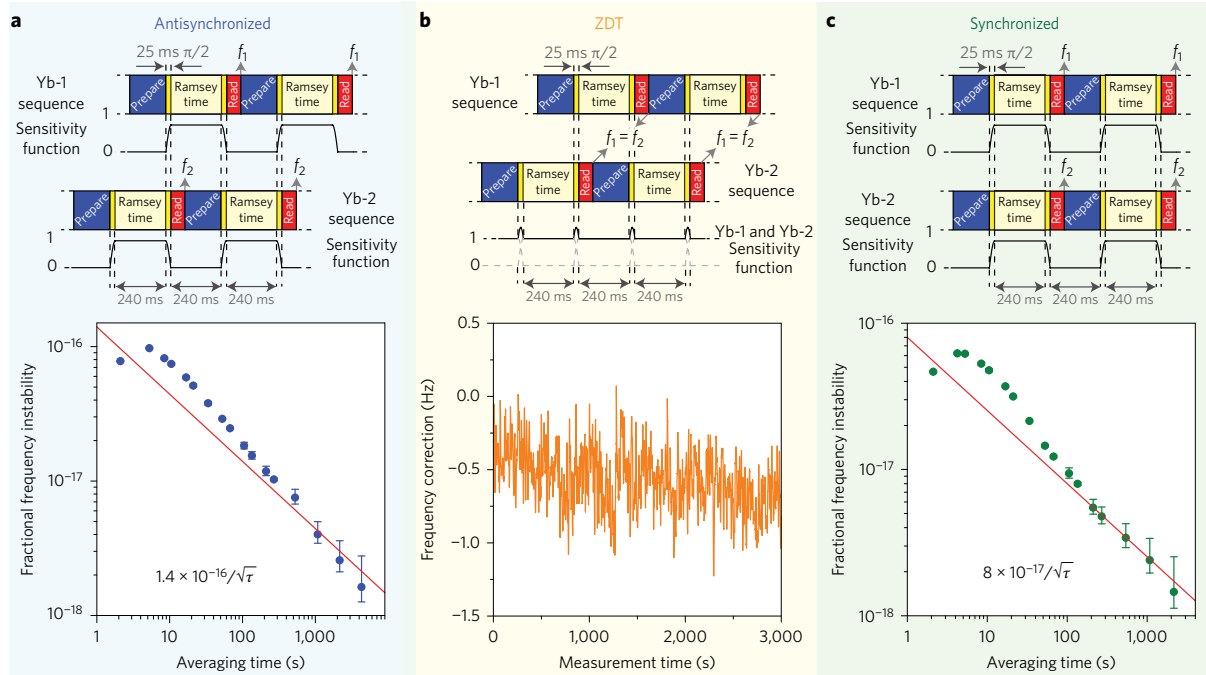


Figure 2 | Timing sequence, sensitivity function and instability measurement for the three schemes studied here. a, The atomic systems are interrogated antisynchronously and the corrections applied independently to their respective AOMs. The Allan deviation of the AOMs frequency difference $\Delta f(t) \equiv f_1(t) - f_2(t)$ results in a measured combined clock instability of $2.0 \times 10^{-16}/\sqrt{\tau}$, which corresponds to a single clock instability of $<1.4 \times 10^{-16}/\sqrt{\tau}$ (see Table 1 and Methods). **b,** In the ZDT configuration, the frequency correction derived from the interrogation of one system is applied phase-continuously during the interrogation of the second system, such that the clock laser interrogates atoms without interruption by cycling between Yb-1 and Yb-2 and is corrected every half of the cycle time, eliminating the source of the Dick effect. Yb-1 and Yb-2 form a composite system, with a shared frequency correction (stabilizing the free-running clock laser to the composite system) of $f_1(t) = f_2(t)$. **c,** Synchronized spectroscopy offers a method to evaluate the instability of the ZDT operation since the OLO noise is common-mode rejected, virtually eliminating the Dick effect. The measured synchronized instability of a single system is $8 \times 10^{-17}/\sqrt{\tau}$. In the ZDT scheme, the observed stability will be improved by $\sqrt{2}$ because the atomic measurements and OLO corrections accumulate twice as often, leading to a ZDT clock instability of $6 \times 10^{-17}/\sqrt{\tau}$. All displayed error bars correspond to a statistical confidence interval of 1σ .

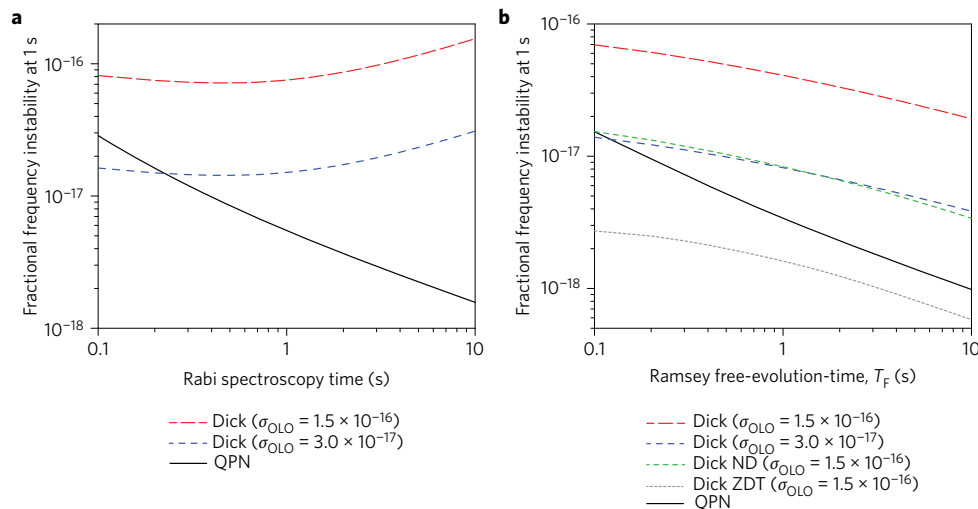


Figure 3 | Computed Dick and QPN instability at 1 s assuming an atom number of 10,000. a, The contribution of the Dick effect is evaluated as a function of Rabi spectroscopy time (dead time fixed to 240 ms) for the measured cavity flicker frequency instability of 1.5×10^{-16} and for a prospective improved cavity with flicker frequency instability of 3.0×10^{-17} . Note that for Rabi spectroscopy, as the OLO flicker frequency noise is aliased, the Dick limit can get worse at longer spectroscopy times. For comparison, the QPN limit is displayed for the Rabi scheme. **b,** Here the Dick instability is evaluated for Ramsey spectroscopy as a function of free-evolution-time, T_F , for the case of cavity flicker frequency instability of 1.5×10^{-16} and 3.0×10^{-17} , both with a fixed dead time of 240 ms. The Dick effect is also calculated for repeated Ramsey spectroscopy using non-destructive (ND) atomic state detection assuming 100 consecutive measurements with 15 ms readout time, a cavity flicker frequency instability of 1.5×10^{-16} and a fixed initial dead time of 240 ms. The Dick instability is also evaluated for Ramsey ZDT for a fixed duty cycle of 50%. The QPN limit for Ramsey spectroscopy is displayed for comparison. The duration of the $\pi/2$ pulses is fixed to 25 ms. Dick noise is calculated generally, according to published methods¹. Note that to operate the clocks with the longest spectroscopy times displayed in the figures requires next generation OLO instability, such as that indicated by the blue dashed curve or using techniques highlighted in Fig. 4.

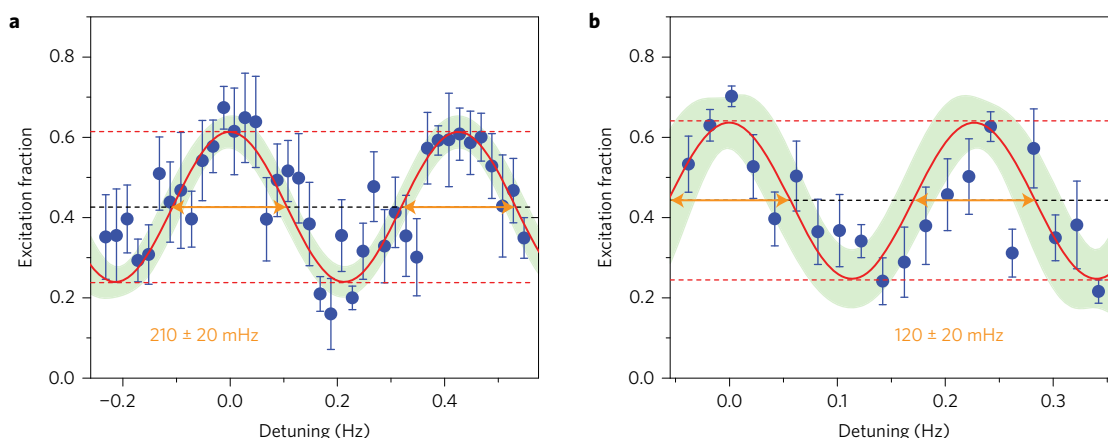


Figure 4 | Long interrogation Ramsey spectroscopy with the OLO pre-stabilized by one (fast) atomic system. The fast atomic system has cycle and free-evolution-times of 240 ms and 110 ms, respectively. To demonstrate the repeatability of these narrow line spectra, here we show the average of seven consecutive laser detuning sweeps. The measured atomic excitation versus detuning is shown by blue circles. The experimental data are fit to a sinusoid to yield the best estimate of the fringe linewidth and contrast (the fit is the red solid line, with the 95% confidence band indicated by the green shading). **a**, Ramsey spectroscopy with the pre-stabilized OLO for a free-evolution-time on the second (slower) atomic system of 2.4 s, leading to a (Fourier-limited) fringe linewidth of 210 ± 20 mHz with 40% contrast. **b**, Here the free-evolution-time for Ramsey spectroscopy on the slower system is 4 s, corresponding to a (Fourier-limited) fringe linewidth of 120 ± 20 mHz with 40% contrast. The linewidths extracted in **a** and **b** are in excellent agreement with their respective Fourier limits of 208 mHz and 125 mHz. The error bars correspond to a statistical confidence interval of 1σ .

time-dependent sensitivity function of each atomic system, both individually suffer from Dick noise. However, because interrogation is performed with a single OLO in a synchronized fashion, the Dick noise is correlated and common-mode rejected in the comparison between the two atomic ensembles. As a result, the synchronized measurement between the two systems and the ZDT clock are sensitive to the same noise processes, as displayed in Table 1, and thus the synchronized measurement can be used to experimentally evaluate the ZDT clock. The resulting synchronized measurement stability is shown in Fig. 2c, averaging down as $8 \times 10^{-17}/\sqrt{\tau}$. For the observed white frequency noise process, the ZDT clock is $\sqrt{2}$ more stable than the synchronized measurement because it accumulates atomic measurements and OLO corrections twice as fast, yielding a ZDT instability of $6 \times 10^{-17}/\sqrt{\tau}$. With the Dick noise suppressed, it is now possible to reach an instability level of 1×10^{-18} in a mere few thousand seconds, an order of magnitude faster than previous clock stability demonstrations^{10–15}.

Beyond reducing the Dick noise, two atomic systems can also be combined in alternate configurations to decrease QPN. Recent proposals use one system in a succession of short interrogation periods to pre-stabilize the OLO such that a second system can then be interrogated over a longer period than the OLO coherence would otherwise permit^{26,27}. Figure 4 displays an experimental step towards one such scheme with the OLO pre-stabilized on one atomic system to increase the interrogation time up to 2.4 s and 4 s on the second atomic system. This leads to Fourier-limited Ramsey fringes with linewidths of 210 ± 20 mHz and 120 ± 20 mHz respectively, with a contrast of 40%. This corresponds to $Q > 4 \times 10^{15}$, the highest observed in an optical lattice clock system. The longer interrogation time and higher Q thus affords reduced QPN (see equation (1)). Because this approach fails to eliminate dead time, its inherent Dick noise suppression is modest compared with that of the ZDT configuration. Therefore, either the ZDT configuration or the long interrogation scheme could be optimal, depending on the relative magnitude of Dick noise and QPN. Hypothetically, if atomic phase correlations/entanglement could be established between two atomic ensembles in a ZDT configuration, the OLO phase could be continuously tracked, fundamentally improving the noise averaging process and thus clock stability.

We have demonstrated a universal optical clock architecture that eliminates Dick noise by combining two atomic ensembles to realize ZDT operation. Clock stability is derived from the atomic system,

rather than relying on OLO coherence. By so doing, we have observed unprecedented clock stability, enabling very high precision with averaging times that are much shorter than were previously possible. With OLO-induced noise removed, optical lattice clocks can reach a performance given by atomic detection noise and its fundamental QPN limit. Attention can thus turn to reducing QPN, as well as spin-squeezing techniques that enable performance beyond the standard quantum limit^{28,29}. The improved stability and reduced measurement time demonstrated here greatly enhance atomic clock utility in tests of fundamental physics, opening the door to 10^{-19} -level timekeeping precision. Furthermore, because of the relaxed requirements on OLO performance, this scheme can reduce the total complexity of state-of-the-art optical clocks, extending their usability outside the laboratory.

Methods

Methods and any associated references are available in the [online version of the paper](#).

Received 16 June 2016; accepted 17 October 2016;
published online 28 November 2016

References

- Dick, G. J. Local oscillator induced instabilities in trapped ion frequency standards. In *Proc. Precise Time and Time Interval Meeting* (ed. Sydnor, R. L.) 133–147 (US Naval Observatory, 1987).
- Santarelli, G. *et al.* Frequency stability degradation of an oscillator slaved to a periodically interrogated atomic resonator. *IEEE Trans. Ultra. Ferro. Freq. Cont.* **45**, 887–894 (1998).
- Dick, G. J., Prestage, J. D., Greenhall, C. A. & Maleki, L. Local oscillator induced degradation of medium-term stability in passive atomic frequency standards. In *Proc. 22nd Precise Time and Time Interval Meeting* (ed. Sydnor, R. L.) 487–508 (NASA, 1990).
- Ludlow, A. D., Boyd, M. M., Ye, J., Peik, E. & Schmidt, P. O. Optical atomic clocks. *Rev. Mod. Phys.* **87**, 637–701 (2015).
- Poli, N., Oates, C. W., Gill, P. & Tino, G. M. Optical atomic clocks. *Riv. Nuovo Cimento* **36**, 555–624 (2013).
- Itano, W. M. *et al.* Quantum projection noise-population fluctuations in 2-level systems. *Phys. Rev. A* **47**, 3554–3570 (1993).
- Chou, C. W., Hume, D. B., Rosenband, T. & Wineland, D. J. Optical clocks and relativity. *Science* **329**, 1630–1633 (2010).
- Derevianko, A. & Pospelov, M. Hunting for topological dark matter with atomic clocks. *Nat. Phys.* **10**, 933–936 (2014).
- Arvanitaki, A., Huang, J. & Van Tilburg, K. Searching for dilation dark matter with atomic clocks. *Phys. Rev. D* **91**, 015015 (2015).

10. Jiang, Y. Y. *et al.* Making optical atomic clocks more stable with 10^{-16} -level laser stabilization. *Nat. Photonics* **5**, 158–161 (2011).
11. Hinkley, N. *et al.* An atomic clock with 10^{-18} instability. *Science* **341**, 1215–1218 (2013).
12. Nicholson, T. L. *et al.* Systematic evaluation of an atomic clock at 2×10^{-18} total uncertainty. *Nat. Commun.* **6**, 6896 (2015).
13. Häfner, S. *et al.* 8×10^{-17} fractional laser frequency instability with a long room-temperature cavity. *Opt. Lett.* **40**, 2112–2115 (2015).
14. Al-Masoudi, A., Dörscher, S., Häfner, S., Sterr, U. & Lisdat, C. Noise and instability of an optical lattice clock. *Phys. Rev. A* **92**, 063814 (2015).
15. Nemitz, N. *et al.* Frequency ratio of Yb and Sr clocks with 5×10^{-17} uncertainty at 150 seconds averaging time. *Nat. Photonics* **10**, 258–261 (2016).
16. Takamoto, M., Takano, T. & Katori, H. Frequency comparison of optical lattice clocks beyond the Dick limit. *Nat. Photonics* **5**, 288–292 (2011).
17. Cole, G. D., Zhang, W., Martin, M. J., Ye, J. & Aspelmeyer, M. Tenfold reduction of Brownian noise in optical interferometry. *Nat. Photonics* **7**, 644–650 (2013).
18. Harry, G. M. *et al.* Titania-doped tantala/silica coatings for gravitational-wave detection. *Classical Quant. Grav.* **24**, 405–415 (2007).
19. Kessler, T. *et al.* A sub-40-mHz-linewidth laser based on a silicon single-crystal optical cavity. *Nat. Photonics* **6**, 687–692 (2012).
20. Poli, N. *et al.* A transportable strontium optical lattice clock. *Appl. Phys. B* **117**, 1107–1116 (2014).
21. Bondarescu, R. *et al.* Ground-based optical atomic clocks as a tool to monitor vertical surface motion. *Geophys. J. Int.* **191**, 1770–1774 (2015).
22. Lisdat, C. *et al.* A clock network for geodesy and fundamental science. *Nat. Commun.* **7**, 12443 (2016).
23. Schiller, S. *et al.* Einstein gravity explorer—a medium-class fundamental physics mission. *Exp. Astron.* **23**, 573–610 (2009).
24. Westergaard, P. G., Lodewyck, J. & Lemonde, P. Minimizing the Dick effect in an optical lattice clock. *IEEE Trans. Ultra. Ferro. Freq. Cont.* **57**, 623–628 (2010).
25. Biedermann, G. W. *et al.* Zero-dead-time operation of interleaved atomic clocks. *Phys. Rev. Lett.* **111**, 170802 (2013).
26. Kohlhaas, R. *et al.* Phase locking a clock oscillator to a coherent atomic ensemble. *Phys. Rev. X* **5**, 021011 (2015).
27. Borregaard, J. & Sørensen, A. S. Efficient atomic clocks operated with several atomic ensembles. *Phys. Rev. Lett.* **111**, 090802 (2013).
28. Wineland, D. J., Bollinger, J. J., Itano, W. M., Moore, F. L. & Heinzen, D. J. Spin squeezing and reduced quantum noise in spectroscopy. *Phys. Rev. A* **46**, R6797–R6800 (1992).
29. Leroux, I. D., Schleier-Smith, M. H. & Vuletić, V. Implementation of cavity squeezing of a collective atomic spin. *Phys. Rev. Lett.* **104**, 073602 (2010).

Acknowledgements

The authors acknowledge the Defense Advanced Research Projects Agency (DARPA) Quantum Assisted Sensing and Readout (QuASAR) programme, the NASA Fundamental Physics programme and the National Institute of Standards and Technology for financial support. R.C.B. acknowledges support from the National Research Council Research Associateship programme. We also thank T. Fortier, F. Quinlan and S. Diddams for femtosecond optical frequency comb measurements.

Author contributions

M.S., R.C.B., W.F.M., R.J.F., G.M., D.N. and A.D.L. carried out the instability measurements. M.S. and A.D.L. constructed the clock laser. W.F.M., T.H.Y. and A.D.L. contributed to the optimization of the clock laser performance. J.A.S. constructed the DDS system for precise cavity drift compensation. R.C.B., N.H., T.H.Y., W.F.M., R.J.F., G.M. and A.D.L. were responsible for the operation of Yb-1 and Yb-2 systems and the phase noise cancellation. K.B. contributed to the evaluation of the instability budget. C.W.O. and A.D.L. supervised this work. All authors contributed to the final manuscript.

Additional information

Supplementary information is available in the [online version of the paper](#). Reprints and permissions information is available online at www.nature.com/reprints. Correspondence and requests for materials should be addressed to A.D.L.

Competing financial interests

The authors declare no competing financial interests.

Methods

OLO. The clock laser is based on a quantum dot laser at 1156 nm amplified and frequency stabilized on a high-finesse Fabry–Perot cavity with a length of 29 cm. The power storage time of the reference cavity is 270 μ s, corresponding to a finesse of 877,000. The radius of curvature of each mirror is 10.5 m, forming a $1/e^2$ intensity beam diameter on the mirrors of 1.34 mm, which averages the Brownian noise of the dielectric mirrors over a large area. The theoretical estimate of the thermal noise floor is 7×10^{-17} . The frequency instability of the clock laser has been measured using the atomic transition as an independent frequency discriminator at the fractional level of $\leq 1.5 \times 10^{-16}$ in the averaging time interval 1–1,000 s. This measurement provides an upper limit since it also includes atomic detection noise. The high finesse allows us to passively reduce the technical instability due to residual amplitude modulation of the phase modulator to $\leq 2 \times 10^{-17}$ in the averaging time interval 1–100 s. The reference cavity is actively temperature stabilized at the null-coefficient-of-thermal-expansion temperature of 35 °C. Three layers of nested in-vacuum thermal radiation shields provide passive thermal insulation with an estimated characteristic response time of a few days. The drift of the cavity has been measured using the atomic transition as a reference on a timescale of one year. During this interval a constant drift of -35 mHz s^{-1} has been observed and linearly compensated with residual nonlinear deviations not exceeding 1 mHz s^{-1} in one day. The sign and the value of the drift is compatible with the creeping of the ultralow-expansion glass spacer. The subharmonic light is frequency doubled to 578 nm through a single pass nonlinear wave guide, providing 5 mW power available for each atomic system.

Ytterbium atomic system. The experimental sequence¹¹ begins by laser slowing and loading into a six-beam magneto-optical trap (MOT) on the spectrally broad (28 MHz) 1S_0 – 1P_1 transition, lasting 80 ms. Our laser slowing process forgoes a typical Zeeman slower in favour of increased atomic flux due to the closer proximity of the atomic oven to the MOT³⁰. Magneto-optic trapping is then switched to the narrow (183 kHz) 1S_0 – 3P_1 transition and the cooling proceeds in three (~20 ms) steps where the laser detuning is set to be progressively lower power and less red-detuned from resonance ultimately producing atomic temperatures of 5–10 μ K. The number of atoms trapped, influencing the relevant quantum projection noise, is 5,000 for Yb-1 and 10,000 for Yb-2. Atomic state preparation is then performed in ~10 ms by optically pumping into either one of the two 1S_0 Zeeman substates. There is a 20 ms delay between optical pumping and spectroscopy that allows for the magnetic field to stabilize. Spectroscopy on the 1S_0 – 3P_0 transition is carried out in both the Lamb–Dicke and well-resolved sideband regimes, eliminating Doppler and recoil effects³¹. After spectroscopy, atomic populations in both the 1S_0 ground and 3P_0 excited electronic states are measured using laser fluorescence shelving detection^{32–34}. The excitation signal, normalized against atom number, is used to stabilize the OLO frequency onto resonance with the lattice-trapped atoms. The choice of Ramsey spectroscopy maximizes the line Q factor for a given spectroscopy time. Indeed, the Fourier-limited linewidth for Ramsey spectroscopy is about 1.6 \times narrower than that for Rabi spectroscopy.

Both atomic systems, Yb-1 and Yb-2, trap ultracold ytterbium in a one-dimensional optical lattice from the same laser source operating at the ‘magic’ wavelength, where Stark shifts from the lattice confinement are matched for both atomic states used for the frequency standard (1S_0 and 3P_0)^{35,36}. The lattice laser frequency is held to the magic value by stabilization to a reference Fabry–Perot cavity, resulting in variations of the lattice Stark shift at a negligible level. Its absolute frequency is occasionally measured with an optical frequency comb. The lattice standing wave in Yb-1 is generated by simple retroreflection of an incident laser, while that for Yb-2 utilizes an enhancement cavity to generate optical power buildup of more than 100 \times the incident laser power and thus enabling use of a large cavity mode diameter to increase the trapping volume. In this work, trap depths of 25 μ K and 40 μ K are employed respectively for Yb-1 and Yb-2.

Rejection of aliased noise. In the time domain, each half of the interleaved, zero-dead-time clock remains sensitive to the Dick effect. However, because the same OLO pulse serves as the first Ramsey pulse in one system and the second Ramsey pulse in the other, the effect of the aliased noise in the two systems has the same magnitude but opposite sign³⁷. Thus when added together, the Dick noise of the two systems effectively cancels out. In order for this suppression to work effectively, OLO noise must be correlated between the two atomic ensembles. For this reason, phase

noise that originates from optical path fluctuations between the OLO and the atomic reference frame, given by the standing wave of each optical lattice, must be actively compensated with an acousto-optic modulator^{38,39}. Using a Mach–Zehnder interferometer, we measured this compensation to be effective at $\leq 2 \times 10^{-17}$ instability in 1 s, which can be further improved. To ensure that no π -radian optical phase shifts occur between Ramsey spectroscopy pulses (due to the 2π ambiguity of the round-trip phase detection process) some OLO light remains on during the Ramsey free-evolution-time. This light is far-detuned from the atomic transition to prevent excitation, and enables the active phase stabilizer to maintain phase continuity between Ramsey pulses.

For Dick suppression to work well, the Ramsey pulses delivered to the two atomic systems must be matched in timing and shape. The Ramsey pulse overlap is realized at the microsecond level. Furthermore, there is no discernible difference between the square OLO pulses to the two systems, at the 0.1% level. Finally, because each atomic interrogation remains sensitive to a relatively large first-order Zeeman shift, differential magnetic field fluctuations between the two atomic systems must be maintained below the milligauss level. These requirements are important for both the ZDT clock and the synchronized measurements between two atomic systems used to assess ZDT performance.

To amplify the observed Dick suppression achieved in the synchronized measurements and possibly in the ZDT clock, we intentionally added white frequency noise onto the OLO while leaving the other operational parameters of the clock unchanged. The noise amplitude was sufficient to increase the antisynchronized measurement instability to $7 \times 10^{-16}/\sqrt{\tau}$, while the synchronized measurement remained below $1.5 \times 10^{-16}/\sqrt{\tau}$. With this rejection factor, under normal OLO noise conditions, we can expect the Dick contribution to be rejected in synchronized measurements to at least below $3 \times 10^{-17}/\sqrt{\tau}$, well below the measured instability.

Single clock instability in the antisynchronized measurement. We estimate the single clock instability in the antisynchronized measurement by dividing the instability of the measured frequency difference by $\sqrt{2}$. This is appropriate for most noise processes, which are uncorrelated between systems. However, in the antisynchronized configuration, Dick noise between the two systems is correlated and requires a linear sum. The fact that some noise in the measured frequency difference adds linearly and other noise adds in quadrature complicates the deduction of the instability contributed by a single clock to a measurement. To conservatively account for correlation of Dick noise in the antisynchronized measurement, the estimated Dick noise in Table 1 is multiplied by $\sqrt{2}$. Following similar arguments, the reported single clock instability for the antisynchronized case ($< 1.4 \times 10^{-16}/\sqrt{\tau}$) represents an upper limit.

References

- Oates, C. W., Bondu, F., Fox, R. W. & Hollberg, L. A diode-laser optical frequency standard based on laser-cooled Ca atoms: sub-kilohertz spectroscopy by optical shelving. *Eur. J. Phys. D* **7**, 449–460 (1999).
- Dicke, R. H. The effect of collisions upon the Doppler width of spectral lines. *Phys. Rev.* **89**, 472–473 (1953).
- Nagourney, W., Sandberg, J. & Dehmelt, H. Shelved optical electron amplifier: observation of quantum jumps. *Phys. Rev. Lett.* **56**, 2797–2799 (1986).
- Sauter, Th., Neuhauser, W., Blatt, R. & Toschek, P. E. Observation of quantum jumps. *Phys. Rev. Lett.* **57**, 1696–1698 (1986).
- Bergquist, J. C., Hulet, R. G., Itano, W. M. & Wineland, D. J. Observation of quantum jumps in a single atom. *Phys. Rev. Lett.* **57**, 1699–1702 (1986).
- Ye, J., Kimble, H. J. & Katori, H. Quantum state engineering and precision metrology using state-insensitive light traps. *Science* **320**, 1734–1738 (2008).
- Katori, H., Takamoto, M., Pal’chikov, V. G. & Ovsiannikov, V. D. Ultrastable optical clock with neutral atoms in an engineered light shift trap. *Phys. Rev. Lett.* **91**, 173005 (2003).
- Meunier, M. *et al.* Stability enhancement by joint phase measurements in a single cold atomic fountain. *Phys. Rev. A* **90**, 063633 (2014).
- Ma, L. S., Jungner, P., Ye, J. & Hall, J. L. Delivering the same optical frequency at 2 places - accurate cancellation of phase noise introduced by an optical-fiber or other time-varying path. *Opt. Lett.* **19**, 1777–1779 (1994).
- Falke, S., Misera, M., Sterr, U. & Lisdat, C. Delivering pulsed and phase stable light to atoms of an optical clock. *Appl. Phys. B* **107**, 301–311 (2012).